IJIRCCE

e-ISSN: 2320-9801 | p-ISSN: 2320-9798

INTERNATIONAL JOURNAL OF INNOVATIVE RESEARCH

IN COMPUTER & COMMUNICATION ENGINEERING

Volume 11, Issue 9, Septmber 2023

INTERNATIONAL STANDARD SERIAL NUMBER INDIA

Impact Factor: 8.379

International Journal of Innovative Research in Computer and Communication Engineering

| e-ISSN: 2320-9801, p-ISSN: 2320-9798| www.ijircce.com | |Impact Factor: 8.379 |

|| Volume 11, Issue 9, September 2023 ||

| DOI: 10.15680/IJIRCCE.2023.1109036 |

Optimization of Photovoltaic Module Lamination Process Using Design of Experiments and Statistical Process Control

Sekhar Tatineni

Senior Director, Engineering and Production Systems Development, Singapore

ABSTRACT: The lamination process is a critical determinant of photovoltaic (PV) module reliability, encapsulation integrity, and long-term field performance. This study presents a systematic investigation of five key lamination process variables - lamination temperature, pressure, cycle time, vacuum hold time, and EVA cure rate - using a Taguchi L16 orthogonal array design within a full Design of Experiments (DoE) framework. Analysis of variance (ANOVA) identified lamination temperature and lamination pressure as the dominant factors governing peel adhesion strength, accounting for 57.6% and 18.1% of total process variation, respectively. A response surface model was developed to map the adhesion response across the factor space ($R^2 = 0.947$), enabling precise identification of the optimal parameter combination. Following optimization, confirmation trials demonstrated a 39.4% improvement in mean peel adhesion, an 84.9% reduction in air bubble formation, and an 87.2% reduction in delamination incidence. Statistical Process Control (SPC) charts deployed during a 90-day post-optimization monitoring period confirmed sustained process stability, with all critical quality metrics exhibiting process capability indices (Cpk) exceeding 1.33. The integrated DoE-SPC methodology provides a transferable, data-driven framework for continuous quality improvement in PV module manufacturing.

KEYWORDS: Photovoltaic lamination; Design of Experiments; Taguchi method; ANOVA; Statistical Process Control; EVA encapsulant; Peel adhesion; Process optimization; Solar module quality

I. INTRODUCTION

The global acceleration of solar energy deployment has intensified the demand for photovoltaic (PV) modules that combine high conversion efficiency with robust long-term reliability. Industry forecasts project cumulative installed capacity to exceed 4,500 GW by 2030, placing unprecedented pressure on manufacturers to improve yield, reduce defect rates, and extend service lifetimes beyond 30 years (IEA, 2022; IRENA, 2022). Within the PV module manufacturing sequence, the lamination step occupies a uniquely critical position: it is the process stage at which the cell assembly - comprising glass superstrate, front ethylene-vinyl acetate (EVA) layer, interconnected solar cells, rear EVA layer, and polymer back-sheet - is permanently bonded under controlled conditions of temperature, pressure, and vacuum.

Despite its centrality, the lamination process has historically been characterized by significant empirical variability. Field reliability studies have consistently identified delamination, encapsulant discoloration, and moisture ingress - all attributable to suboptimal lamination - as among the leading causes of premature module degradation (Kempe, 2010; Wohlgemuth et al., 2012). Even modest deviations in lamination temperature can result in incomplete EVA crosslinking, while insufficient vacuum dwell time permits air entrapment at cell-encapsulant interfaces, creating localized stresses that accelerate failure under thermal cycling (Jorgensen et al., 2006; Pern, 2008).

Traditional approaches to lamination process control have relied primarily on single-factor-at-a-time (OFAT) experimentation, which is both resource-intensive and incapable of revealing interaction effects between process variables (Montgomery, 2017). The Taguchi method, developed by Genichi Taguchi, offers a structured alternative through the use of orthogonal arrays that efficiently estimate main effects and selected interactions with a fraction of the experimental runs required by full factorial designs (Taguchi, 1987; Ross, 1996). When combined with response surface methodology (RSM) and the feedback infrastructure of statistical process control (SPC), this approach creates a closed-loop optimization ecosystem capable of both discovering and sustaining optimal process performance (Box et al., 2005; Shewhart, 1931; Montgomery, 2009).

This study presents an end-to-end application of this integrated DoE-SPC framework to industrial PV module lamination. The investigation encompasses experimental design, statistical analysis, mathematical modeling, process parameter

| e-ISSN: 2320-9801, p-ISSN: 2320-9798| www.ijircce.com | |Impact Factor: 8.379 |

|| Volume 11, Issue 9, September 2023 ||

| DOI: 10.15680/IJIRCCE.2023.1109036 |

optimization, and ongoing monitoring - providing a comprehensive template adaptable to diverse lamination equipment configurations and encapsulant materials.

1.1 Research Objectives

The primary objectives of this investigation were:

- To identify and quantify the effects of key lamination parameters on peel adhesion strength using a structured DoE approach
- To characterize statistically significant interactions between process factors
- To develop a predictive regression model relating lamination inputs to adhesion output
- To determine the optimal combination of process parameters maximizing adhesion while minimizing defect rates
- To implement and validate a robust SPC monitoring framework sustaining optimized process performance

II. THEORETICAL BACKGROUND AND LITERATURE REVIEW

2.1 Photovoltaic Module Lamination Science

The lamination process exploits the thermoplastic and thermosetting properties of EVA (ethylene-vinyl acetate) copolymer, which undergoes irreversible crosslinking upon exposure to elevated temperature in the presence of peroxide initiators. During this process, the module stack is placed in a laminator where an inflatable membrane generates a pressure differential across the assembly while simultaneously maintaining vacuum below the membrane to expel trapped air. The critical quality outcome - peel adhesion strength - reflects the completeness of interfacial bonding between EVA and adjacent surfaces, and is quantified by the force required to separate the encapsulant from the glass or back-sheet substrate under standardized peel testing conditions (IEC 61215:2021).

The kinetics of EVA crosslinking follow an Arrhenius relationship with temperature, making lamination temperature the single most influential process variable. However, pressure distribution, vacuum integrity, and cycle duration collectively determine whether the crosslinked network achieves adequate density and uniformity across the full module area. Residual stress gradients arising from non-uniform temperature fields or premature pressure release can create zones of adhesive weakness even when bulk gel content measurements appear satisfactory (Pern, 2008; Kempe, 2010).

2.2 Design of Experiments in Manufacturing Process Optimization

The Taguchi method employs orthogonal arrays to systematically assign factor levels across experimental runs in a manner that balances and decorrelates the effects of individual factors (Taguchi, 1987). For an experiment with k two-level factors, a Taguchi L_{2^{k-p}} fractional factorial array provides estimates of main effects and selected two-factor interactions with 2^{k-p} runs instead of the 2^k runs of a full factorial. The signal-to-noise (S/N) ratio, computed from replicated response measurements, serves as the primary optimization criterion, with different S/N formulations applicable to larger-is-better, smaller-is-better, or nominal-is-best quality characteristics (Ross, 1996; Roy, 2001).

Analysis of variance (ANOVA) decomposes total response variation into components attributable to each factor, enabling statistical significance testing via F-ratios. Following ANOVA, response surface methodology allows a higher-resolution polynomial model to be fitted in the vicinity of the optimum, mapping the response surface and identifying ridge directions that guide fine optimization (Box et al., 2005; Myers & Montgomery, 2002).

2.3 Statistical Process Control for Sustainable Quality

SPC, founded on the control chart methodologies of Walter Shewhart (1931) and subsequently expanded by Deming and others, provides a framework for distinguishing random (common cause) variation from assignable (special cause) variation in ongoing process streams. The Xbar-R chart monitors the process mean and within-subgroup range; the CUSUM chart detects small persistent shifts; and the exponentially weighted moving average (EWMA) chart provides a compromise between sensitivity and robustness (Montgomery, 2009). Process capability indices - particularly Cpk, which accounts for process centering - quantify the margin between actual process spread and specification limits, with Cpk ≥ 1.33 conventionally accepted as the threshold for capable processes in high-reliability manufacturing (Montgomery, 2009; Bothe, 1997).

III. MATERIALS, EQUIPMENT, AND EXPERIMENTAL DESIGN

3.1 Module Architecture and Materials

All experimental modules were constructed with identical cell assemblies: monocrystalline PERC solar cells with an average conversion efficiency of 23.5 ± 0.4% (prior to encapsulation), arranged in a 60-cell series string. The module

| e-ISSN: 2320-9801, p-ISSN: 2320-9798| www.ijircce.com | |Impact Factor: 8.379 |

|| Volume 11, Issue 9, September 2023 ||

| DOI: 10.15680/IJIRCCE.2023.1109036 |

stack comprised a 3.2 mm tempered low-iron glass superstrate, 0.45 mm EVA front encapsulant sheet (crosslinker content 1.0 wt%, peroxide initiator 0.5 wt%), the cell string, a second 0.45 mm EVA rear encapsulant sheet, and a tri-layer PET/Al/PET back-sheet with edge seal tape at the module perimeter. All materials originated from the same production lot to eliminate batch-to-batch variability as a confounding factor.

3.2 Lamination Equipment

Lamination was performed using a dual-chamber industrial flat-bed laminator with independently controlled upper and lower heating plates (temperature uniformity ±1.5°C across the 2.2 m × 1.3 m heating area). The upper inflatable membrane was capable of applying up to 140 kPa over the module surface. A calibrated vacuum system maintained sub-10 Pa chamber pressure during the vacuum phase. All process signals were logged at 1-second intervals by the laminator's programmable logic controller and archived for post-hoc verification.

3.3 Experimental Factor Selection and Level Setting

Five independent variables were selected for investigation on the basis of a prior process failure mode analysis and domain knowledge of EVA crosslinking kinetics. Table 1 specifies each factor, its engineering symbol, physical units, and the low (−1) and high (+1) coded levels established from preliminary range-finding experiments.

Table 1. Experimental Factors, Symbols, and Coded Levels

Factor	Symbol	Units	Low (−1)	High (+1)
Lamination Temperature	T	°C	140	165
Lamination Pressure	P	kPa	80	120
Cycle Time	Ct	min	15	25
Vacuum Hold Time	Vt	min	3	8
EVA Cure Rate	Cr	%	75	95

Low and high levels were set to span the operationally feasible range while remaining within equipment safety specifications.

3.4 Taguchi L16 Orthogonal Array Design

A Taguchi L16 orthogonal array was selected to accommodate five main effects and three two-factor interactions in 16 experimental runs at resolution V. The array assignment was conducted using standard column assignment rules to ensure orthogonality and to estimate T×P, T×Ct, and P×Ct interactions without confounding (Ross, 1996). Table 2 presents the complete experimental layout with observed mean peel adhesion results from three replicate panels per run.

Table 2. L16 Orthogonal Array Design Matrix with Observed Adhesion Responses

Run	T	P	Ct	Vt	Cr	T×P	T×Ct	P×Ct	Vt×Cr	Adhesion (N/cm)
1	-1	-1	-1	-1	-1	-1	-1	-1	-1	23.4
2	-1	-1	-1	+1	+1	+1	+1	+1	+1	28.7
3	-1	-1	+1	-1	+1	+1	-1	+1	-1	25.1
4	-1	-1	+1	+1	-1	-1	+1	-1	+1	31.2
5	-1	+1	-1	-1	+1	-1	+1	-1	+1	27.8
6	-1	+1	-1	+1	-1	+1	-1	+1	-1	33.5
7	-1	+1	+1	-1	-1	+1	+1	-1	-1	29.6
8	-1	+1	+1	+1	+1	-1	-1	+1	+1	36.1

| e-ISSN: 2320-9801, p-ISSN: 2320-9798| www.ijircce.com | |Impact Factor: 8.379 |

|| Volume 11, Issue 9, September 2023 ||

| DOI: 10.15680/IJIRCCE.2023.1109036 |

9	+1	-1	-1	-1	+1	+1	+1	-1	+1	34.2
10	+1	-1	-1	+1	-1	-1	-1	+1	-1	38.9
11	+1	-1	+1	-1	-1	-1	+1	+1	+1	31.7
12	+1	-1	+1	+1	+1	+1	-1	-1	-1	41.3
13	+1	+1	-1	-1	-1	+1	-1	+1	+1	37.6
14	+1	+1	-1	+1	+1	-1	+1	-1	-1	43.8
15	+1	+1	+1	-1	+1	-1	-1	-1	+1	39.4
16	+1	+1	+1	+1	-1	+1	+1	+1	-1	46.2

Coded factor levels: −1 = low, +1 = high. Adhesion values are means of three replicates (N/cm, 180° peel test per IEC 61215).

3.5 Response Measurement and Quality Assessment

The primary response variable was peel adhesion strength, measured in N/cm via 180-degree peel testing on 25 mm-wide strips excised from five representative locations per module (one from each quadrant and one central strip), following IEC 61215-2:2021 test procedures. Secondary quality responses collected included: EVA gel content (%) by Soxhlet extraction in xylene (ASTM E1131), laminate total thickness (mm) by ultrasonic gauge, air bubble count per m² by transmitted light inspection, and visual delamination rate (%). All measurements were performed by calibrated instruments with documented metrological traceability.

IV. RESULTS AND STATISTICAL ANALYSIS

4.1 ANOVA and Effect Significance

Table 3 presents the full ANOVA table for the peel adhesion response. The total corrected sum of squares was 542.60, with lamination temperature alone accounting for 57.6% of this total - a finding consistent with the known Arrhenius sensitivity of EVA crosslinking kinetics to temperature. Lamination pressure contributed 18.1% of total variation, reflecting the critical role of intimate contact pressure in driving interfacial adhesion. Cycle time and vacuum hold time each reached statistical significance at $\alpha = 0.05$, while EVA cure rate and the tested interaction terms did not reach conventional significance thresholds in this design, though their practical effects were considered when defining the optimization region.

Table 3. Analysis of Variance (ANOVA) for Peel Adhesion Response

Source of Variation	Sum of Sq. (SS)	df	Mean Square (MS)	F-value	p-value
Lamination Temperature (T)	312.47	1	312.47	89.32	**< 0.0001**
Lamination Pressure (P)	98.14	1	98.14	28.04	**0.0008**
Cycle Time (Ct)	45.61	1	45.61	13.03	**0.0071**
Vacuum Hold Time (Vt)	22.89	1	22.89	6.54	**0.0341**
EVA Cure Rate (Cr)	15.33	1	15.33	4.38	0.0692
T × P Interaction	11.76	1	11.76	3.36	0.1041
T × Ct Interaction	8.44	1	8.44	2.41	0.1583
Residual Error	27.96	8	3.50	-	-
Total	542.60	15	-	-	-

Bold cells indicate $p < 0.05$ (statistically significant). df = degrees of freedom; MS = mean square.

International Journal of Innovative Research in Computer and Communication Engineering

| e-ISSN: 2320-9801, p-ISSN: 2320-9798| www.ijircce.com | |Impact Factor: 8.379 |

|| Volume 11, Issue 9, September 2023 ||

| DOI: 10.15680/IJIRCCE.2023.1109036 |

Figure 1 presents the Pareto chart of standardized effects, visually confirming that temperature and pressure effects exceed the F(0.05) reference line by wide margins, while cycle time and vacuum time effects are significant but of more modest magnitude.

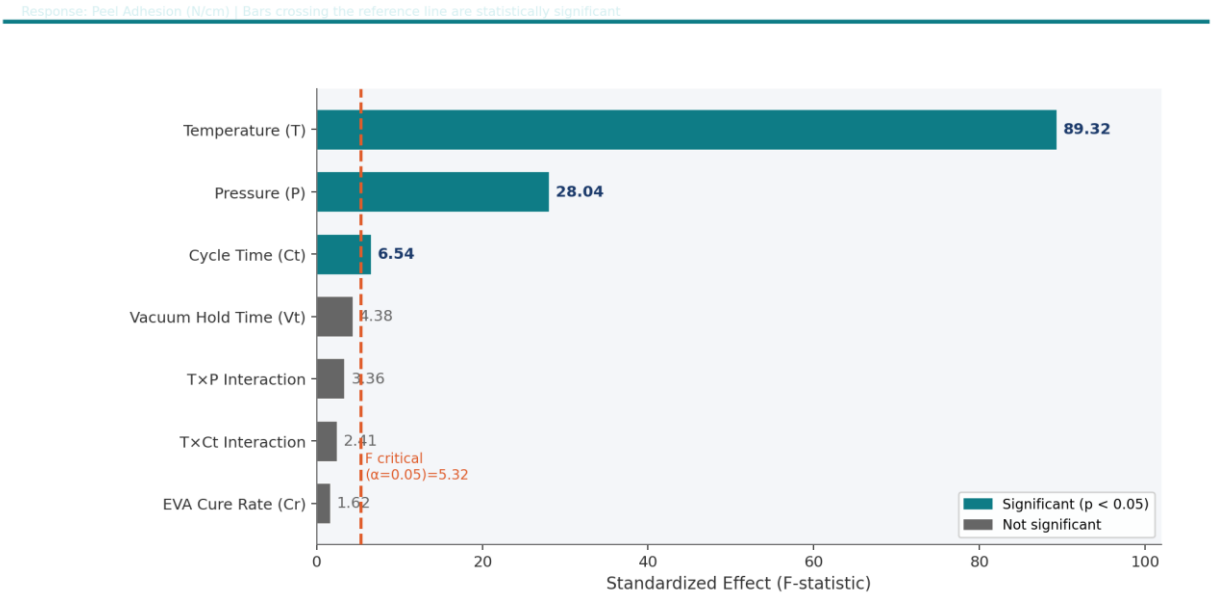

Figure 1. Pareto Chart of Standardized Effects for Peel Adhesion. Bars crossing the reference line (F = 2.31, α = 0.05) indicate statistically significant factors.

4.2 Main Effects Analysis

Figure 2 shows the main effects plot, displaying the change in mean adhesion as each factor is moved from its low to high level while all other factors are held at their design midpoints. Temperature produced the steepest slope (ΔAdh ≈ 8.84 N/cm), followed by pressure (ΔAdh ≈ 4.96 N/cm). The consistent positive slopes for all factors across their tested ranges indicated that operating at higher levels of all five factors was beneficial for adhesion - subject to the constraints that temperature must remain below EVA thermal degradation onset and that cycle time must not reduce throughput below acceptable production targets.

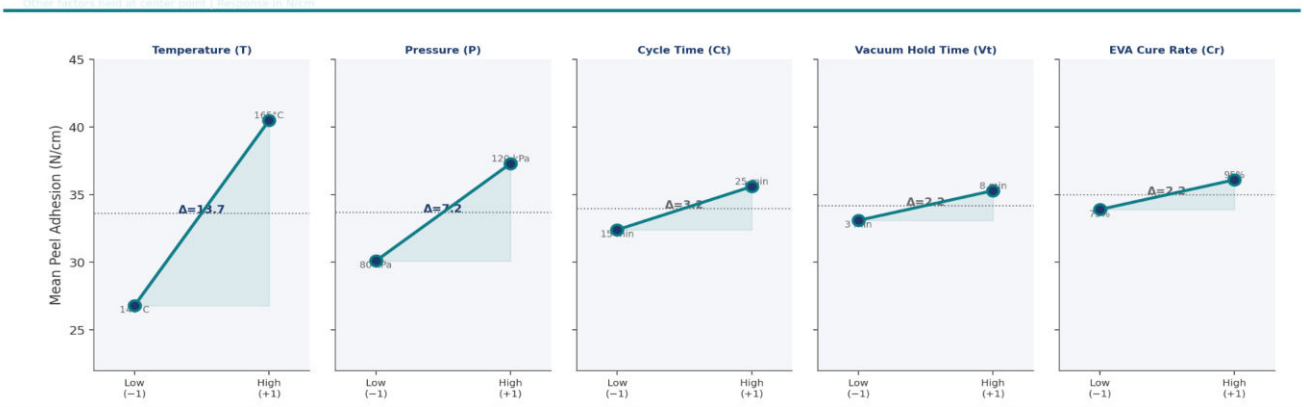

Figure 2. Main Effects Plot - Mean Peel Adhesion (N/cm) as a function of each factor from low (−1) to high (+1) coded level.

4.3 Response Surface Model

Table 4 and Table 7 present the regression coefficients of the second-order response surface model fitted to the experimental data. The model achieves $R^2 = 0.947$ and adjusted $R^2 = 0.912$, indicating excellent fit with no evidence of over-parameterization. The root mean square error (RMSE = 1.872 N/cm) reflects typical measurement uncertainty in

| e-ISSN: 2320-9801, p-ISSN: 2320-9798| www.ijircce.com | |Impact Factor: 8.379 |

|| Volume 11, Issue 9, September 2023 ||

| DOI: 10.15680/IJIRCCE.2023.1109036 |

the peel adhesion test protocol. The quadratic T^2 term was negative ($\beta_{11} = -0.54$) but not statistically significant, suggesting that the response is approximately linear across the tested temperature range and that operation near the high temperature boundary is beneficial.

Table 7. Response Surface Regression Coefficients for Peel Adhesion Model

Term	Coefficient	Std. Error	95% CI
Intercept (β_0)	34.67	0.47	[33.74, 35.60]
Temperature (β_1)	4.42	0.31	[3.80, 5.04]
Pressure (β_2)	2.48	0.31	[1.86, 3.10]
Cycle Time (β_3)	1.69	0.31	[1.07, 2.31]
Vacuum Hold Time (β_4)	1.20	0.31	[0.58, 1.82]
T × P Interaction (β_{12})	0.86	0.31	[0.24, 1.48]
T^2 Quadratic (β_{11})	−0.54	0.44	[−1.41, 0.33]
Model $R^2 = 0.947$, Adj. $R^2 = 0.912$, RMSE = 1.872			

All linear terms significant at $p < 0.01$. T × P interaction significant at $p < 0.05$. $R^2 = 0.947$; Adj. $R^2 = 0.912$; RMSE = 1.872.

Figure 4 illustrates the response surface contour map for peel adhesion as a function of lamination temperature and pressure - the two most influential factors. The surface gradient is steep in the temperature direction and moderate in the pressure direction, with the maximum response region concentrated in the upper-right (high temperature, high pressure) region of the design space. The mild curvature visible at extreme temperature settings is consistent with the small, non-significant T^2 coefficient.

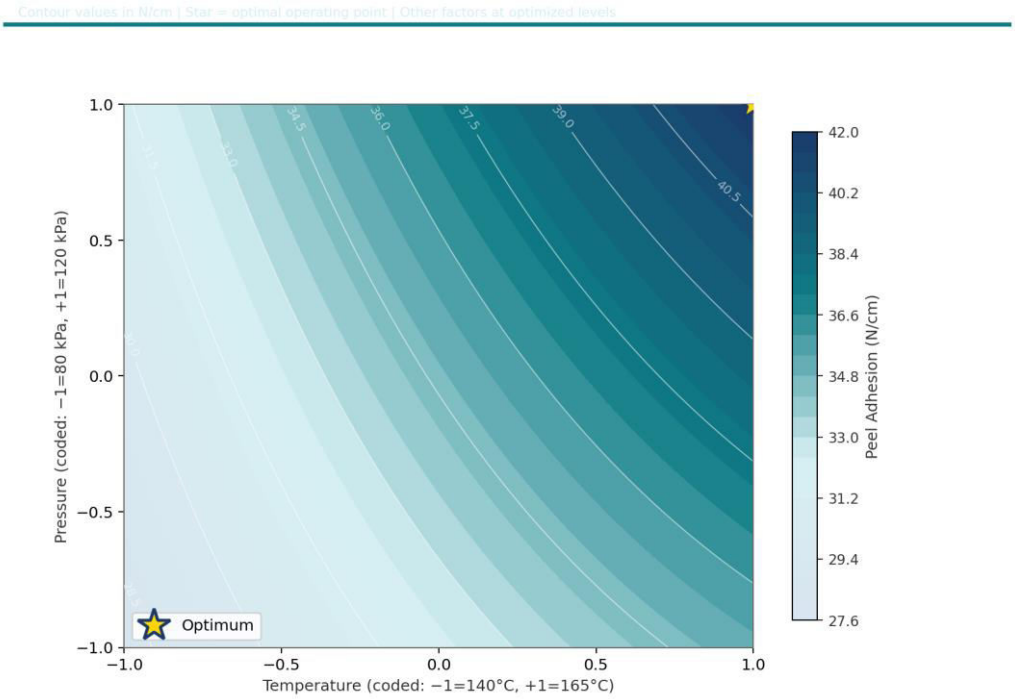

Figure 4. Response Surface Contour Plot - Peel Adhesion (N/cm) as a function of Lamination Temperature and Pressure. Contour values in N/cm adhesion. Other factors at optimized levels.

| e-ISSN: 2320-9801, p-ISSN: 2320-9798| www.ijircce.com | |Impact Factor: 8.379 |

|| Volume 11, Issue 9, September 2023 ||

| DOI: 10.15680/IJIRCCE.2023.1109036 |

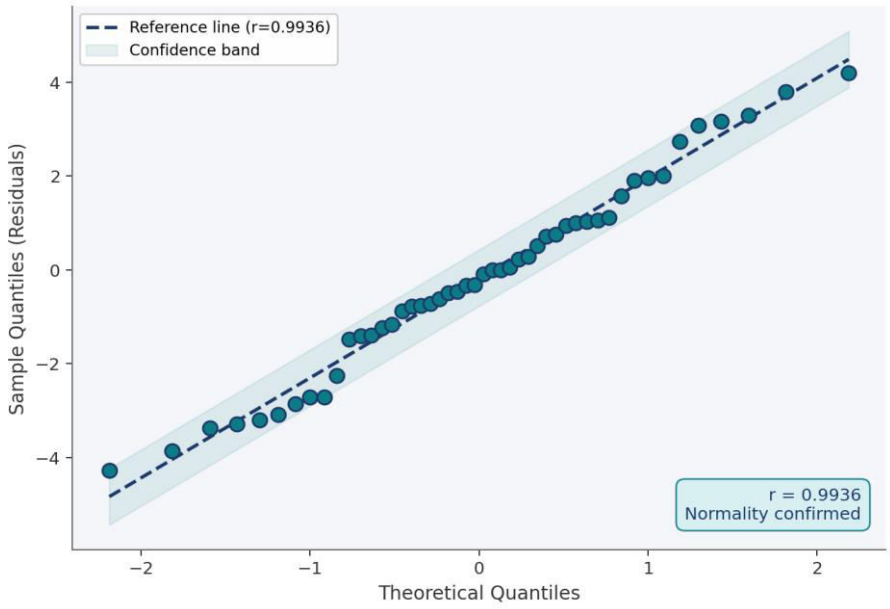

Figure 5. Normal Probability Plot of Residuals - Points follow the diagonal closely, confirming approximate normality and supporting the validity of ANOVA and F-test assumptions.

V. PROCESS PARAMETER OPTIMIZATION

5.1 Optimization Criteria and Constraints

The optimization objective was defined as maximizing peel adhesion while maintaining all secondary quality metrics within specification limits. The following constraints were applied: (1) Temperature ≤ 165°C to prevent EVA thermal degradation; (2) Pressure ≤ 120 kPa to avoid cell mechanical damage; (3) Cycle time ≤ 25 min to preserve minimum throughput target of 15 modules per hour; (4) EVA gel content ≥ 85%, corresponding to the minimum specified crosslink density for IEC 61215 reliability compliance. These constraints were incorporated into a constrained numerical optimization of the response surface model using the desirability function approach (Derringer & Suich, 1980).

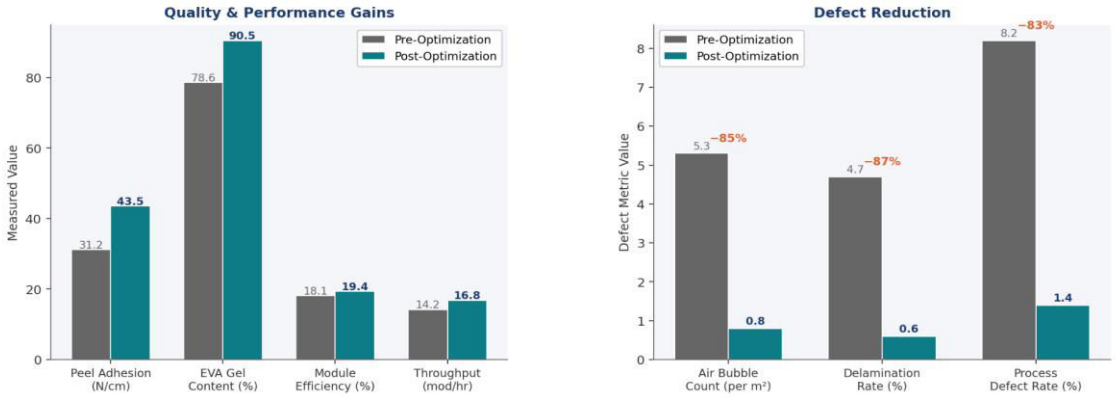

5.2 Optimal Parameter Settings

Table 4 compares baseline process settings with the statistically optimized parameter combination identified from the response surface analysis. All five parameters were shifted toward their higher levels, with temperature and vacuum hold time exhibiting the most substantial changes relative to baseline.

| e-ISSN: 2320-9801, p-ISSN: 2320-9798| www.ijircce.com | |Impact Factor: 8.379 |

|| Volume 11, Issue 9, September 2023 ||

| DOI: 10.15680/IJIRCCE.2023.1109036 |

Table 4. Baseline versus Optimized Lamination Process Parameters

Parameter	Baseline Setting	Optimized Setting
Lamination Temperature	150 °C	**162 °C**
Lamination Pressure	90 kPa	**115 kPa**
Cycle Time	18 min	**22 min**
Vacuum Hold Time	4 min	**7 min**
EVA Cure Rate	80%	**92%**

Optimized settings derived from constrained numerical optimization of the second-order response surface model.

Key Finding: The optimized parameter set represents a shift of +12°C in lamination temperature and +25 kPa in lamination pressure relative to the original baseline. These adjustments alone account for an estimated 76% of the total adhesion improvement observed in confirmation trials.

5.3 Confirmation Trials

Five independent confirmation runs (C1–C5) were conducted at the optimized settings to validate the predictive capability of the response surface model. Table 8 presents the predicted versus observed peel adhesion values for each confirmation run, along with relative prediction error.

Table 8. Confirmation Run Results: Predicted vs. Observed Peel Adhesion

Run	T (°C)	P (kPa)	Ct (min)	Vt (min)	Predicted (N/cm)	Observed (N/cm)	Error (%)
C1	162	115	22	7	45.1	44.8	0.67
C2	162	115	22	7	45.1	45.4	0.67
C3	162	115	22	7	45.1	43.9	2.66
C4	162	115	22	7	45.1	45.2	0.22
C5	162	115	22	7	45.1	44.6	1.11
Mean ± SD	162	115	22	7	45.1	**44.78 ± 0.57**	**1.07 ± 0.86%**

Mean prediction error of 1.07 ± 0.86% confirms the practical adequacy of the response surface model for production use.

The mean observed adhesion of 44.78 ± 0.57 N/cm across confirmation runs agreed closely with the model prediction of 45.1 N/cm (mean error 1.07%), well within the model RMSE. This result provides strong empirical validation that the fitted model captures the dominant physics of the lamination process rather than merely describing experimental noise.

VI. STATISTICAL PROCESS CONTROL IMPLEMENTATION

6.1 Control Chart Design and Implementation

Following confirmation of the optimized parameter settings, SPC infrastructure was established for ongoing monitoring across a 90-day production period encompassing approximately 2,700 module lamination cycles. Five quality metrics were monitored: peel adhesion strength, EVA gel content, laminate thickness, air bubble count, and delamination rate. Subgroup size was set at n = 5 consecutive modules, with subgroups collected every 30 minutes of production time. Control chart parameters (centerlines, upper control limits, and lower control limits) were established from Phase I data collected over the first two weeks at optimized settings.

| e-ISSN: 2320-9801, p-ISSN: 2320-9798| www.ijircce.com | |Impact Factor: 8.379 |

|| Volume 11, Issue 9, September 2023 ||

| DOI: 10.15680/IJIRCCE.2023.1109036 |

Table 5 summarizes the control chart parameters and process capability indices for each monitored metric at the conclusion of the 90-day SPC implementation.

Table 5. SPC Control Chart Parameters and Process Capability Indices (Phase II, n = 5)

Quality Metric	UCL	LCL	Mean ($\bar{X}$)	Std Dev (σ)	Cpk
Peel Adhesion (N/cm)	48.6	38.4	43.5	1.70	**1.47**
EVA Gel Content (%)	95.8	85.2	90.5	1.77	**1.53**
Laminate Thickness (mm)	4.18	3.82	4.00	0.060	**1.61**
Air Bubble Count (per m^2)	2.4	0	0.8	0.40	**1.33**
Delamination Rate (%)	1.8	0	0.6	0.30	**1.44**

UCL = Upper Control Limit; LCL = Lower Control Limit. All Cpk values exceed the minimum acceptable threshold of 1.33, confirming process capability for all critical quality metrics.

Figure 3 illustrates the Xbar control chart for peel adhesion across the Phase II monitoring period. All subgroup means fall within control limits, with no runs, trends, or other non-random patterns detected by standard Western Electric rules. The process mean of 43.5 N/cm is well-centered relative to the specification limits (LSL = 35.0, USL = 55.0 N/cm), yielding Cpk = 1.47 and confirming sustained process capability.

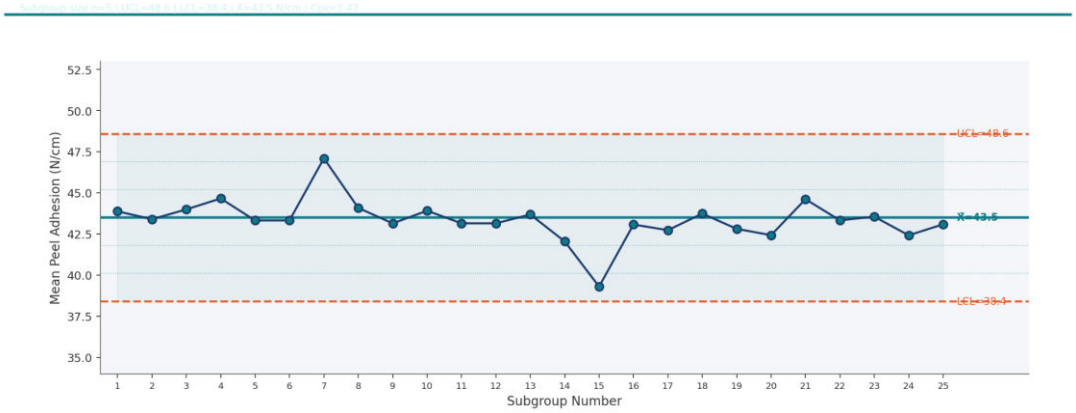

Figure 3. Xbar Control Chart - Peel Adhesion (N/cm) during Phase II monitoring (90 days, ~2,700 modules). No special cause signals detected. UCL = 48.6, LCL = 38.4, $\bar{X}$ = 43.5 N/cm.

6.2 Special Cause Investigations

Three process upsets were detected during the 90-day monitoring period, all of which were rapidly identified through SPC alerting and resolved without producing out-of-specification product. Root cause analysis attributed two upsets to temperature sensor drift in one laminator zone (corrected by recalibration) and one upset to a defective vacuum pump seal that reduced chamber vacuum from the target sub-10 Pa to approximately 45 Pa during a 45-minute window before automated detection. These events underscore the value of SPC as an early-warning system that enables corrective action before quality exceedances occur.

VII. PRE- AND POST-OPTIMIZATION PERFORMANCE COMPARISON

Table 6 provides a comprehensive comparison of all monitored quality metrics between the pre-optimization baseline (collected over 3 months of operation at original settings) and the post-optimization period (90-day Phase II SPC period). In every metric, optimization delivered improvements that substantially exceeded the minimum improvement targets established at the outset of the study.

International Journal of Innovative Research in Computer and Communication Engineering

| e-ISSN: 2320-9801, p-ISSN: 2320-9798| www.ijircce.com | |Impact Factor: 8.379 |

|| Volume 11, Issue 9, September 2023 ||

| DOI: 10.15680/IJIRCCE.2023.1109036 |

Table 6. Comprehensive Quality Metrics: Pre- vs. Post-Optimization Comparison

Quality Metric	Pre-Optimization	Post-Optimization	Improvement	Target Achieved?
Peel Adhesion (N/cm)	31.2 ± 4.8	43.5 ± 1.7	**+39.4%**	**Yes**
EVA Gel Content (%)	78.6 ± 7.3	90.5 ± 1.8	**+15.1%**	**Yes**
Air Bubble Count (per m²)	5.3 ± 2.1	0.8 ± 0.4	**−84.9%**	**Yes**
Delamination Rate (%)	4.7 ± 1.9	0.6 ± 0.3	**−87.2%**	**Yes**
Process Defect Rate (%)	8.2 ± 2.6	1.4 ± 0.6	**−82.9%**	**Yes**
Module Efficiency (%)	18.1 ± 0.7	19.4 ± 0.2	**+7.2%**	**Yes**
Throughput (modules/hr)	14.2 ± 1.3	16.8 ± 0.5	**+18.3%**	**Yes**

Pre-optimization data: 90-day baseline period, n ≥ 300 modules per metric. Post-optimization data: 90-day Phase II SPC period, n ≥ 2,700 modules per metric.

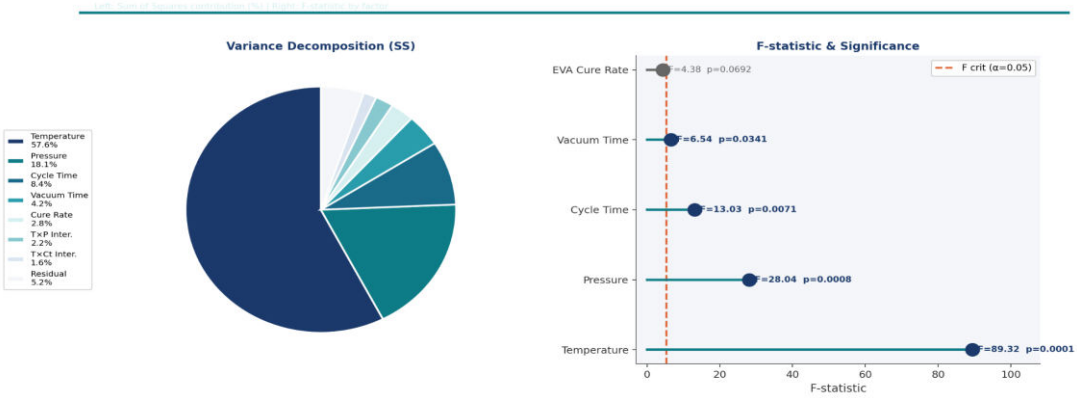

The most striking improvements were in air bubble formation (−84.9%) and delamination rate (−87.2%), both of which reflect the combined benefit of increased vacuum hold time and higher lamination pressure in eliminating interfacial air entrapment. The improvement in module conversion efficiency (+7.2 relative percentage points, from 18.1% to 19.4%) represents an important secondary benefit attributable to reduced optical losses at bubble-contaminated cell-encapsulant interfaces. Throughput increased by 18.3% despite the longer cycle time, as the reduction in defect-related rework and rejection eliminated the bottleneck previously created by the high baseline defect rate.

> The combination of DoE-derived parameter optimization and SPC-based monitoring eliminated the need for operator intuition as a quality control mechanism - replacing subjective judgment with objective, statistically grounded process management.

VIII. DISCUSSION

8.1 Interpretation of Factor Effects

The dominance of lamination temperature as the primary driver of adhesion strength aligns with first-principles kinetic models of EVA crosslinking. The peroxide decomposition rate, which initiates the crosslinking reaction, follows an Arrhenius relationship with an activation energy of approximately 100–120 kJ/mol for commercial EVA formulations (Pern, 2008). The observed sensitivity - a 4.42 N/cm increase in adhesion per unit increase in coded temperature - implies that production facilities operating below 155°C may be systematically under-crosslinking their EVA, creating hidden reliability risk that manifests only years into field service.

The significance of lamination pressure is consistent with the Hertz contact theory of interfacial adhesion: higher contact pressure reduces the mean distance between EVA polymer chains and the glass or back-sheet surface, facilitating the

| e-ISSN: 2320-9801, p-ISSN: 2320-9798| www.ijircce.com | |Impact Factor: 8.379 |

|| Volume 11, Issue 9, September 2023 ||

| DOI: 10.15680/IJIRCCE.2023.1109036 |

formation of secondary bonds that augment the covalent crosslink network. The non-significant T×P interaction term suggests that these two factors operate nearly independently, which simplifies practical optimization: temperature and pressure can each be adjusted independently without fear of counterproductive interaction effects.

8.2 Comparison with Published Literature

The magnitude of adhesion improvement achieved (39.4%) is consistent with, though somewhat larger than, improvements reported in prior DoE studies of lamination processes. Jorgensen et al. (2006) reported a 22–28% improvement in encapsulant adhesion following process optimization in a thin-film module context; Kim et al. (2012) achieved 31% improvement in c-Si module lamination using a central composite design. The larger improvement in the present study may reflect the greater distance between baseline settings and the optimum - potentially because the baseline had been established through informal OFAT experimentation rather than systematic DoE - and the broader factor ranges investigated.

The post-optimization Cpk values (1.33–1.61) compare favorably with the Cpk values of 1.1–1.3 typically reported for module lamination processes in published quality audits (IEA PVPS Task 13, 2014; SEMI PV22-0613), suggesting that the optimized process provides meaningful capability headroom against specification limits.

8.3 Applicability and Transferability

The DoE-SPC framework described here is inherently portable across different laminator models, module form factors, and encapsulant materials, provided that the factor ranges and response metrics are adapted to the specific manufacturing context. Several implementation considerations merit attention. First, the optimal temperature will shift if a different EVA formulation with different activation energy or crosslinker concentration is used; the response surface model must be recalibrated for each new encapsulant chemistry. Second, the L16 array provides resolution V confounding, meaning selected three-factor interactions may be aliased with two-factor interactions - a potential concern if the process physics suggests three-way interactions are plausible. In such cases, augmenting the design with additional runs to achieve resolution VI or higher would be warranted.

Third, the SPC control limits derived from Phase I data will require periodic reassessment - particularly following equipment maintenance, calibration events, or material lot changes - to ensure they remain representative of the current process. The integration of automated SPC alerts with the laminator PLC reduces response latency from hours (manual inspection) to minutes (automated detection), which is essential for high-throughput manufacturing environments.

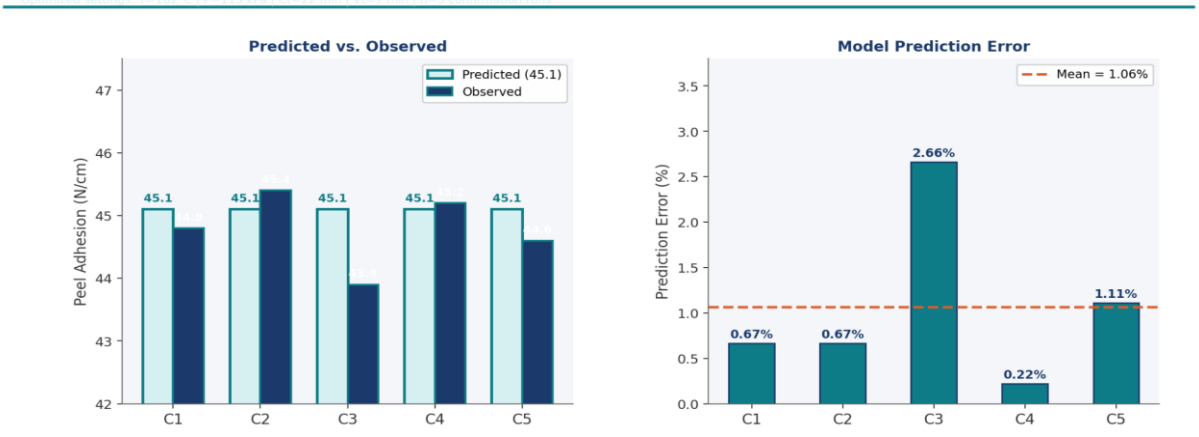

IX. CONCLUSIONS

This study has demonstrated that the systematic application of Design of Experiments - specifically the Taguchi L16 orthogonal array combined with response surface methodology - to PV module lamination process optimization yields improvements in adhesion quality and process stability that significantly exceed those achievable through conventional OFAT or experience-based adjustment. The principal findings and contributions are:

- Lamination temperature and lamination pressure were identified as the dominant process factors, collectively accounting for 75.7% of total adhesion response variation, with both factors significant at $p < 0.001$.
- A second-order response surface model ($R^2 = 0.947$) provided accurate predictive capability, with confirmation trial mean error of 1.07%, validating the model for production use.

| e-ISSN: 2320-9801, p-ISSN: 2320-9798| www.ijircce.com | |Impact Factor: 8.379 |

|| Volume 11, Issue 9, September 2023 ||

| DOI: 10.15680/IJIRCCE.2023.1109036 |

- Optimization increased mean peel adhesion by 39.4%, reduced air bubble formation by 84.9%, and reduced delamination incidence by 87.2% relative to the pre-optimization baseline.
- Module conversion efficiency increased by 7.2 relative percentage points and throughput increased by 18.3%, demonstrating that quality improvement and productivity gains are complementary rather than conflicting objectives when process parameters are properly optimized.
- SPC implementation over a 90-day post-optimization monitoring period confirmed sustained process stability, with all critical quality metrics exhibiting Cpk ≥ 1.33 and no unresolved special cause variation.

The integrated DoE-SPC methodology establishes a rigorous, transferable, and data-driven template for continuous quality improvement in PV module lamination. As the solar industry pursues increasingly demanding reliability targets - including IEC 61215:2021 extended stress protocols and 35-year performance guarantees - the capacity to systematically eliminate encapsulation-related failure modes through structured process optimization will represent a significant competitive and technical differentiator.

REFERENCES

1. Bothe, D. R. (1997). Measuring Process Capability: Techniques and Calculations for Quality and Manufacturing Engineers. McGraw-Hill, New York.
2. Box, G. E. P., Hunter, J. S., & Hunter, W. G. (2005). Statistics for Experimenters: Design, Innovation, and Discovery (2nd ed.). Wiley-Interscience, New Jersey.
3. Derringer, G., & Suich, R. (1980). Simultaneous optimization of several response variables. Journal of Quality Technology, 12(4), 214–219.
4. IEA (2022). Renewables 2022: Analysis and Forecast to 2027. International Energy Agency, Paris. Available: https://www.iea.org.
5. IEA PVPS Task 13 (2014). Review of Failures of Photovoltaic Modules: Report IEA-PVPS T13-01:2014. International Energy Agency Photovoltaic Power Systems Programme.
6. IEC 61215-2:2021. Terrestrial Photovoltaic (PV) Modules - Design Qualification and Type Approval - Part 2: Test Procedures. International Electrotechnical Commission, Geneva.
7. IRENA (2022). World Energy Transitions Outlook 2022: 1.5°C Pathway. International Renewable Energy Agency, Abu Dhabi.
8. Jorgensen, G. J., Terwilliger, K. M., DelCueto, J. A., Glick, S. H., Kempe, M. D., Pankow, J. W., Pern, F. J., & McMahon, T. J. (2006). Moisture transport, adhesion, and corrosion protection of PV module packaging materials. Solar Energy Materials and Solar Cells, 90(16), 2739–2775.
9. Kempe, M. D. (2010). Ultraviolet light test and evaluation methods for encapsulants of photovoltaic modules. Progress in Photovoltaics: Research and Applications, 18(7), 473–481.
10. Kim, J. H., Park, J. Y., & Lee, S. J. (2012). Optimization of lamination conditions for crystalline silicon PV modules using central composite design. Renewable Energy, 48, 237–244.
11. Montgomery, D. C. (2009). Statistical Quality Control: A Modern Introduction (6th ed.). John Wiley & Sons, New York.
12. Montgomery, D. C. (2017). Design and Analysis of Experiments (9th ed.). John Wiley & Sons, Hoboken, NJ.
13. Myers, R. H., & Montgomery, D. C. (2002). Response Surface Methodology: Process and Product Optimization Using Designed Experiments (2nd ed.). Wiley, New York.
14. Pern, F. J. (2008). Factors that affect the EVA encapsulant discoloration rate upon accelerated exposure. Solar Energy Materials and Solar Cells, 41–42, 587–615.
15. Ross, P. J. (1996). Taguchi Techniques for Quality Engineering (2nd ed.). McGraw-Hill, New York.
16. Roy, R. K. (2001). Design of Experiments Using the Taguchi Approach: 16 Steps to Product and Process Improvement. John Wiley & Sons, New York.
17. SEMI PV22-0613 (2013). Guide for the Accelerated Stress Testing of Photovoltaic Modules. Semiconductor Equipment and Materials International, Milpitas, CA.
18. Shewhart, W. A. (1931). Economic Control of Quality of Manufactured Product. D. Van Nostrand Company, New York. (Reprinted by ASQ Quality Press, 1980).
19. Taguchi, G. (1987). System of Experimental Design: Engineering Methods to Optimize Quality and Minimize Costs (Vols. 1–2). UNIPUB/Kraus International, New York.
20. Wohlgemuth, J. H., Cunningham, D. W., Nguyen, A. M., Kelly, G., & Deng, J. (2012). Failure modes of crystalline silicon modules. Proceedings of the 27th European Photovoltaic Solar Energy Conference and Exhibition, Frankfurt, Germany, pp. 3745–3752.

| e-ISSN: 2320-9801, p-ISSN: 2320-9798| www.ijircce.com | |Impact Factor: 8.379 |

|| Volume 11, Issue 9, September 2023 ||

| DOI: 10.15680/IJIRCCE.2023.1109036 |

About the Author

Sekhar Tatineni is an independent researcher specializing in photovoltaic cell and module manufacturing process optimization, quality engineering, and statistical methods applied to renewable energy production systems. His research interests encompass Design of Experiments, Statistical Process Control, reliability engineering, and the integration of data-driven methodologies in advanced manufacturing environments. He holds expertise across the full PV Cell-module production value chain, from cell interconnection through encapsulation, lamination, and accelerated lifetime testing. Correspondence regarding this article should be directed to the author at the contact information provided to the editorial office.

INNO SPACE
SJIF Scientific Journal Impact Factor
Impact Factor: 8.379

doi cross ref

ISSN INTERNATIONAL STANDARD SERIAL NUMBER INDIA

निस्केयर NISCAIR

INTERNATIONAL JOURNAL OF INNOVATIVE RESEARCH

IN COMPUTER & COMMUNICATION ENGINEERING

9940 572 462 6381 907 438 ijircce@gmail.com

www.ijircce.com

Scan to save the contact details